Use of mobile aerosol dosimeter to estimate seasonal concentrations of ultrafine particles

A. ILIE[1,2], J. VASILESCU[1], C. TALIANU[1,*], S. ANDREI[1], A. M. DANDOCSI[1], A. V. DANDOCSI[1,3]
[1]*National Institute of Research and Development for Optoelectronics - INOE 2000, 409 Atomistilor St., 077125, Măgurele, Romania*
[2]*Faculty of Geography, University of Bucharest, 1 Nicolae Bălcescu Blvd., 010041, Bucharest, Romania*
[3]*UNST Politehnica of Bucharest, 1-3 Iuliu Maniu Blvd., Bucharest, 061071, Bucharest, Romania*

The study was carried out for Bucharest, Romania, and assessed the ability of aerosol dosimeter measurements to highlight the seasonal and spatial variability of ultrafine particle emissions. For this purpose, a mobile campaign of measurements on the design route was conducted for two distinct periods: May-July 2022 and January-February 2023, during which 15 routes were successfully completed for each period, covering almost a 100 km long route.
The results indicate that the aerosol dosimeter is able to highlight the main sources of ultrafine particle emissions as well as their variability. Thus, for both seasons, the highest concentrations of ultrafine particles were recorded in areas with heavy traffic, such as boulevards and important intersections, which are predominant sources of ultrafine particles in urban environments. Moreover, significant diurnal variations in the concentrations of ultrafine particles were observed, especially in the cold season, with peaks occurring during the morning and evening hours, periods of time associated with household activities and home heating. These results ensure the premise that calibrated and inter-compared aerosol dosimeters can be used in air quality monitoring networks in urban areas as well as in mobile measurement campaigns.

(Received March 21, 2025; accepted August 5, 2025)

Keywords: Aerosol dosimeter, Ultrafine particles, Mobile measurements, Air quality

1. Introduction

Optoelectronics plays a key role in the development and refinement of methods for measuring particulate matter (PM) and providing accurate and rapid solutions for their detection and characterisation. Optoelectronic technologies are based on the interaction between light and particles, using principles such as light scattering, absorption, or attenuation to determine the concentration and size of the particles [1,2]. Devices such as optical particle counters and electrical mobility mass spectrometers equipped with optoelectronic modules allow real-time monitoring of ultrafine particles.

Air pollution with particulate matter is a global problem [3,4], and has adverse effects on human health [3]. Their level measurement is important and necessary for understanding and mitigating the effects on the environment and human health.

The correlation between particle size and possible health consequences is not fully understood and sometimes causes debate [5-7]. For example, Iskandar et al. (2012) [8] determined that pediatric asthma-related hospital admissions were associated with levels of coarse and fine particles. In contrast, Franck et al. (2011) [9] hypothesised that smaller particles exert a more pronounced impact on cardiovascular disease in general.

Ultrafine particles (UFP) are defined as particles with diameters less than 100 nm in urban environments [10]. In some cases, broader definitions (e.g., <300 nm) may be used for specific studies or applications [11,12]. The UFP mainly originates from incomplete combustion like the one generated by cars [10,13,14], but can also arise spontaneously through nucleation processes in ambient air [15]. Nucleation occurs naturally in the atmosphere, although the precursors that initiate this process can come from human or natural sources [16].

In general, concentrations of UFP in the atmosphere are quantified by total particle number concentration or number size distribution. There are currently no regulatory limit values for UFP concentrations, mainly due to insufficient data for epidemiological research. In 2021, the World Health Organization (WHO) acknowledged the necessity of ultrafine particle (UFP) measurement. In 2024, the European Union amended its air quality regulation 2008/50/EG, requiring at least one ultrafine particle measurement site per 5 million inhabitants in areas of anticipated high concentrations and in supersites [17].

Urban air pollution is a serious environmental issue that impacts cities all around the globe, including Romania's capital, Bucharest [18]. Pollutant emissions into the atmosphere present serious health hazards and have an impact on the environment as metropolitan areas continue to develop and become more industrialised. Due to factors such as energy production, industrial activities, and vehicle emissions, air pollution has become a significant issue within the metropolitan areas [19,20]. Due to the emerging needs to monitor or understand the air quality in many European cities, the variability and concentrations of air pollutants are highlighted in these papers: Hamburg, Germany [43], Barcelona, Spain [21], Paris, France [22], Rome, Italy [23], Amsterdam, Netherlands, Antwerp, Belgium, Leicester, and London, United Kingdom [24].

Besides the fixed-location sites to measure air quality variables, in the last decades, the increase of mobile air quality measurements even for research purposes has been noticed. Different mobile platforms, such as bikes [25-27], buses/trams [28], and pedestrians [29-31], are used for mobile measurements. Mobile measurements serve various purposes, such as evaluating individual exposure by using a portable monitor [32,33], evaluating exposure in various modes of transportation [34,35], assessing seasonal and regional variations of air pollutants [36-43], studying spatiotemporal correlation with noise, studying spatial variation in air pollution, and developing and validating air quality models [44-46]. Moreover, it is used to compute high-spatial-resolution maps of air pollution [47,48].

With a mobile platform, it is possible to sample various geographically diverse environments with just a handful of (expensive) monitoring equipment in a constrained amount of time [47]. These platforms, combined with improvements in air monitoring equipment, such as increased portability and time resolution, enable the collection of a wide range of air contaminants in space and time inside a complex urban terrain. On the other hand, temporal aggregation is necessary for mobile measurements to be relevant to the long-term/average exposure since they often only include a brief period of data per street segment. In contrast, although they only cover a small geographic area, fixed sensors and devices cover long-time periods of air quality data that are representative for that site. Therefore, fixed sensor networks offer temporal profiles but are restricted in number, while mobile platforms can cover more sites but require more repetitions throughout time [48].

To guarantee efficient functioning and precise data gathering, mobile mapping and monitoring devices need to fulfil several specific conditions. These conditions include the capacity to operate properly in the face of possible interferences, like vibrations, power supply fluctuations and signal obstructions, and a high frequency of data acquisition rate. Instrumentation suitable for mobile measurements should be lightweight and resistant to vibrations and shocks. Furthermore, they must reliably record high-resolution temporal data and monitor various contaminants; depending on the mobile platform, the monitoring intervals usually range from one to ten seconds [48]. Correlating the gathered data with exact geographic coordinates also requires integration with GPS [47,48].

Mobile monitoring can be conducted in two ways. One approach involves following predetermined routes repeatedly, while the other approach is more opportunistic, with an operator performing measurements during its regular activities without disruption. Mobile monitoring can follow predetermined routes for consistency and comparability or take an opportunistic approach, offering broader coverage but less control over measurement conditions [48].

It's also crucial to remember that detecting PM in environments with high relative humidity is challenging since water condensation affects the results without providing a way to adjust for it [43,48-50].

This study focuses on ultrafine particle variability assessment in Bucharest using the Partector 2 instrument [51], which was operated for a set of 15 mobile measurements during the warm season between May-July 2022, and another set of measurements during the cold season between January and February 2023.

2. Experimental

2.1. Measurement location

The capital city of Romania, Bucharest, is one of Southeast Europe's major cities. It is the nation's biggest metropolis, home to more than 2.1 million people, and a vital centre for political, cultural, and economic activity. With a total area of 240 km^2, the city has an average population density of 9000 people per km^2 [52] situated on the banks of the Dâmbovița River. Bucharest is in the humid continental climatic zone of the mid-latitudes, which has distinct seasons that are characterised by hot summers and cold winters. The climate of Romania is mostly temperate continental, shaped by diverse atmospheric circulation patterns. During the summer and fall months, cyclonic activity predominates, resulting in heightened precipitation and volatile weather conditions. In contrast, winter and spring exhibit anticyclonic conditions, often linked to easterly and southeasterly air masses, leading to drier and more stable weather. [53,54]. Seasonal fluctuation is characteristic for Bucharest, where annual precipitation totals vary from around 600 mm to 700 mm, with the most significant rainfall often occurring in late spring and early summer [55,56]. Due to atmospheric circulation patterns, long-range aerosol transport events such as wildfires and desert dust intrusion from Persia, the Arabian Peninsula, and the Sahara may have an impact on the air quality in Bucharest [57,58]. Nonetheless, the primary sources are local, impacted by the terrain and various wind regimes at the local scale [59].

The mobile measurements starting point is located in Măgurele city, from the premises of Măgurele Center for Atmosphere and Radiation Studies (MARS) near Bucharest [60-63] (Fig. 1). MARS site is part of RADO-Bucharest national facility, part of the pan-European research infrastructure ACTRIS [64] and is dedicated to atmospheric research.

MARS site was used to initially test the mobile equipment and intercompare the measurements with standard instrumentation [60,65].

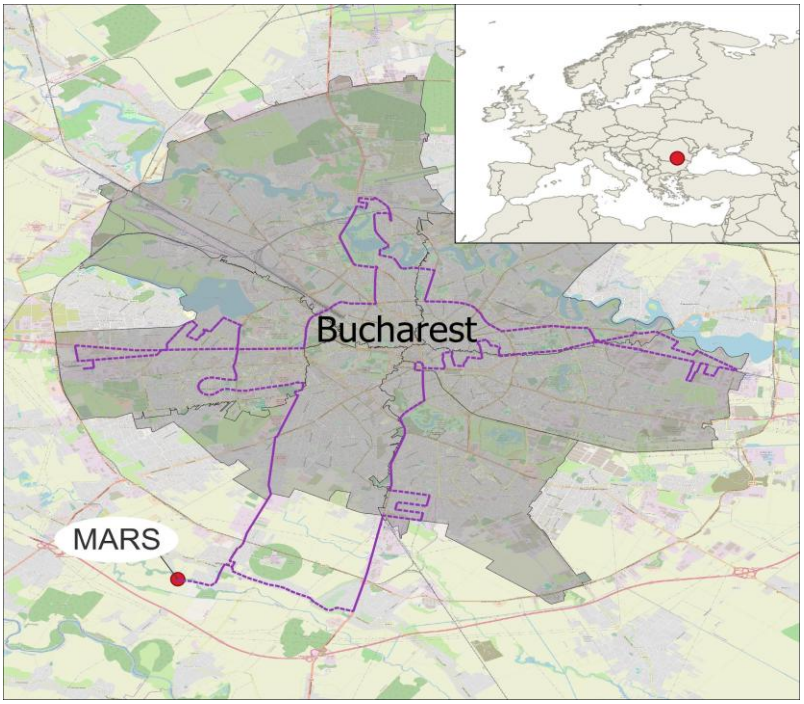

Fig. 1. Map with the measurement route (purple) and the location of the starting point at MARS (colour online)

2.2. Equipment

2.2.1. Naneos Partector 2 - aerosol dosimeter

Naneos Partector 2 [49,57] is a state-of-the-art electronic aerosol dosimeter designed to measure ultrafine particles in the atmosphere. It measures at a frequency of 1 second various parameters related to ultrafine particles ($PM_{0.3}$ - particles with a diameter in the range of 10-300 nm), such as long deposited surface area (LDSA) [µm²/cm³], number concentration [cm^{-3}], total surface area [µm²/cm³], and average particle diameter [nm]. The measurement principle involves charging aerosol particles using a unipolar corona diffusion charger in pulsed mode, generating voltage peaks as charged particles pass through an induction tube. The half peak-to-peak value represents the charge concentration [51], which correlates with LDSA concentration, measurable within ±30% uncertainty [66]. Partector 2 refines this approach with a dual-stage charge measurement system, using an aerosol manipulator to partially remove charged particles before a second induction tube. By analysing the ratio of two measured currents, it estimates the mean particle size, number concentration, and LDSA, similar to other mechanical or electrical aerosol devices [67,68]. For this study, Naneos Partector 2 was used both stationary at the MARS site and during mobile measurement campaigns dedicated to air quality assessment in Bucharest.

2.2.2. Scanning Mobility Particle Sizer (SMPS) spectrometer

The Scanning Mobility Particle Sizer (SMPS) spectrometer is used to continuously measure the size distributions and mass concentration of ultrafine particles as part of the aerosol in-situ ACTRIS component , following the standard CEN/TS-17434 [64]. The SMPS classifies particles according to their electrical mobility using an electric field in a differential electrical mobility classifier [69]. For this study, SMPS was used to measure particle number size distributions in the size range from 10 to 800 nm and mass concentration at the same time as the Partector for several days. The particle concentrations in the same range as the Partector were retrieved and used for intercomparison.

The SMPS operates on the principle of electrical mobility classification principle of aerosol particles followed by optoelectronic detection. The system consists of two primary components: a Differential Mobility Analyser (DMA) and a Condensation Particle Counter (CPC) [69].

In the DMA, particles are first brought to a known charge distribution using a radioactive neutraliser source. After that, the aerosol flow goes through a high-voltage electrostatic classifier. The classifier separates particles based on their electrical mobility, after that the CPC is counting the particle's number concentrations.

The CPC employs an optoelectronic detection mechanism to measure particle concentrations. As the aerosol stream becomes saturated with vapour (e.g., butanol), particles act as nucleation sites for condensation and grow to optically detectable sizes. The enlarged particles pass through a focused laser beam, where light scattering events are detected by a photodetector. Each scattered light pulse corresponds to an individual particle, allowing for real-time quantification [70].

This combination of electrical mobility sizing and optoelectronic detection enables the SMPS to provide high-resolution size distributions of fine particles (including ultrafine), making it particularly suitable for investigating

seasonal variations in urban aerosol concentrations. The optoelectronic components ensure high sensitivity and precision, which is crucial for accurately characterising particle size distributions [69].

2.3. Campaign design

The mobile campaign route was designed using the technique outlined in [48,60,71]. The whole length of this road, accounting for approximately 100 km, included different land uses: commercial, industrial, residential, and mixed-use districts.

In order to characterise a variety of traffic behaviours, the route also contains several street types, such as side streets, less-travelled alleyways, and major thoroughfares with heavy traffic.

The measurement route consists of 40.4 km of primary streets represented by boulevards and major roads, where most traffic takes place, and 33.2 km of secondary streets, typically referring to a type of street that serves to collect traffic from residential, 14.5 km of tertiary streets refers to streets that have lower traffic volumes and serve more localised areas than secondary streets, 12.3 km of residential streets, designed to provide access to homes and residential areas, and 1.1 km of service streets, which are typically access roads to companies and factories [72].

The mobile measurements took place between 5:00 and 13:00 UTC, and its projected length was 8 hours. This time frame was deliberately selected to include two crucial windows of high traffic volume: the first peak hours, which occur between 5:00 and 07:00 UTC, during which residents go to work or school, and the beginning of the second peak, which occurs between 13:00 and 15:00 UTC, during which many people head back home [7]. As a result, the recorded data can depict the variable conditions of the air due to various traffic patterns seen over the day.

We performed the mobile measurements using a passenger automobile and a maximum travel speed of 30 km/h in order to allow the instrument to properly sample the air and to have relevant data on a high spatial resolution as possible street segments.

The mobile measurements were performed exclusively under appropriate weather conditions (without precipitation). These circumstances were necessary to guarantee the consistency and accuracy of the data gathered since precipitation and high humidity have a major impact on particle-related measurements. During the measurements, a dehumidifier was used to ensure that the relative humidity remained below 50%.

The mobile monitoring campaign was carried out in Bucharest for two different time periods of the year. The first-time interval was selected between May and July 2022, which is specific to the warm season, and the second time interval was selected between January and February 2023, corresponding to the specific period of the cold season. During these periods, two sets of identically 15 routes each were successfully completed that ensured full coverage of all potential sources of ultrafine particles in Bucharest. To highlight the seasonal dependence and the type of sources emitting ultrafine particles, rainy and/or windy days were excluded from the measurement campaign. The measurement schedule and the days involved in the campaign are shown in Table 1.

Table 1. List of mobile measurement days

Warm Period			Cold Period		
Date	Start-End [UTC]	Duration	Date	Start-End [UTC]	Duration
04/05/2022	05:30 - 13:10	7h 40m	18/01/2023	06:18 - 12:43	6h 25m
11/05/2022	05:28 - 13:02	7h 33m	19/01/2023	06:17 - 12:15	5h 57m
19/05/2022	05:28 - 12:41	7h 12m	25/01/2023	06:13 - 12:24	6h 11m
26/05/2022	05:31 - 12:48	7h 16m	30/01/2023	06:57 - 12:51	5h 53m
02/06/2022	05:26 - 12:43	7h 17m	01/02/2023	06:18 - 12:29	6h 10m
06/06/2022	05:37 - 12:47	7h 9m	02/02/2023	06:46 - 13:21	6h 35m
07/06/2022	05:18 - 12:00	6h 41m	06/02/2023	06:19 - 11:41	5h 21m
08/06/2022	05:23 - 12:27	7h 4m	07/02/2023	06:28 - 13:18	6h 50m
09/06/2022	05:10 - 12:21	7h 10m	09/02/2023	06:30 - 12:49	6h 18m
14/06/2022	05:19 - 12:11	6h 51m	13/02/2023	06:30 - 12:50	6h 20m
16/06/2022	05:26 - 12:41	7h 14m	14/02/2023	06:42 - 12:50	6h 8m
22/06/2022	05:28 - 12:13	6h 44m	15/02/2023	06:40 - 12:38	5h 58m
29/06/2022	05:32 - 12:02	6h 29m	21/02/2023	06:52 - 12:32	5h 40m
06/07/2022	05:19 - 11:45	6h 25m	22/02/2023	06:34 - 12:51	6h 16m
13/07/2022	05:33 - 12:15	6h 41m	28/02/2023	06:35 - 12:15	5h 40m
Total		105h 34m	Total		91h 48m

2.4. Data processing and analysis

To assure the quality and relevance of the data in this study, it was necessary to apply several data filtering and processing techniques. The algorithms used to analyse and process the data were generated in Python 3.8 using the modules pandas, geopandas, numpy, and seaborn.

For the quality and consistency of the data obtained during the campaign, Naneos Partector 2 aerosol dosimeter data were intercompared with the SMPS data measured in the same conditions. The intercomparison was done using co-located static measurements at MARS. This step was performed before the mobile measurements to assess the degree of agreement between the two instruments and to understand any systematic bias for the mobile aerosol dosimeter. Results are shown in section 3.1.

Rolling averages were initially computed with a window of three values. Moving averages were used on the data to show overall trends and reduce short-term variations. The ratio between each individual value and its matching moving average value was then computed. To lessen the impact of extreme values and noise in the data, a value was deemed an outlier and deleted from the data set if the ratio was larger than 1.5.

Static data in this context describes times when the car was not moving for more than five minutes. These idle times were eliminated since they did not provide any relevant data for campaign analysis. To provide a more accurate and relevant picture of the vehicle's behaviour throughout the campaign, this filtering was done to concentrate the study on the times when the vehicle was moving.

For a more representative assessment of exposure levels, averaging techniques were used to compute mean UFP concentrations over different temporal and spatial scales. Standard deviation calculations were used to quantify data variability and identify potential outliers or anomalous fluctuations. Spatial analysis was conducted using the geopandas Python module [73], enabling the examination of concentration distributions across different areas of Bucharest. Temporal analysis involved the evaluation of UFP trends over different time frames, including daily and seasonal variations. The seasonal variability was evaluated through a comparative analysis of the concentrations of fine particles recorded in the period May-July 2022 (warm season) and in the period January-February 2023 (cold season).

3. Results and discussions

3.1. Intercomparison of measurements

Fig. 2 illustrates the relationship between number concentrations measured by Partector 2 and SMPS during a correlation campaign conducted at the MARS site in July 2022. The linear regression line shows a positive trend, suggesting that overall, the two devices give correlated mass concentration measurements.

The Pearson correlation coefficient ($R = 0.70$) shows a strong relationship between the two data sets, and the coefficient of determination ($R^2 = 0.49$) indicates that 49% of the variation in mass concentration measured by Partector 2 is explained by the SMPS, with the remaining difference attributed to measurement uncertainties and retrieval factors [74], [75].

The main source of these discrepancies comes from the different measurement principles of the two instruments. SMPS estimates number concentration based on particle size distribution using electrical mobility classification. In contrast, Partector 2 determines number concentration based on the total electrical charge of the particles, which makes it more sensitive to the chemical composition and ionisation properties of the aerosols. Thus, the differences between the measurements can be explained by the fact that the same particles can generate different signals in the two instruments. Variations may also result from differences in time resolution, detection efficiency for smaller particles, and instrument response to changing environmental conditions [49], [76]. Nevertheless, both instruments sense the same variability of the number concentrations of UFP.

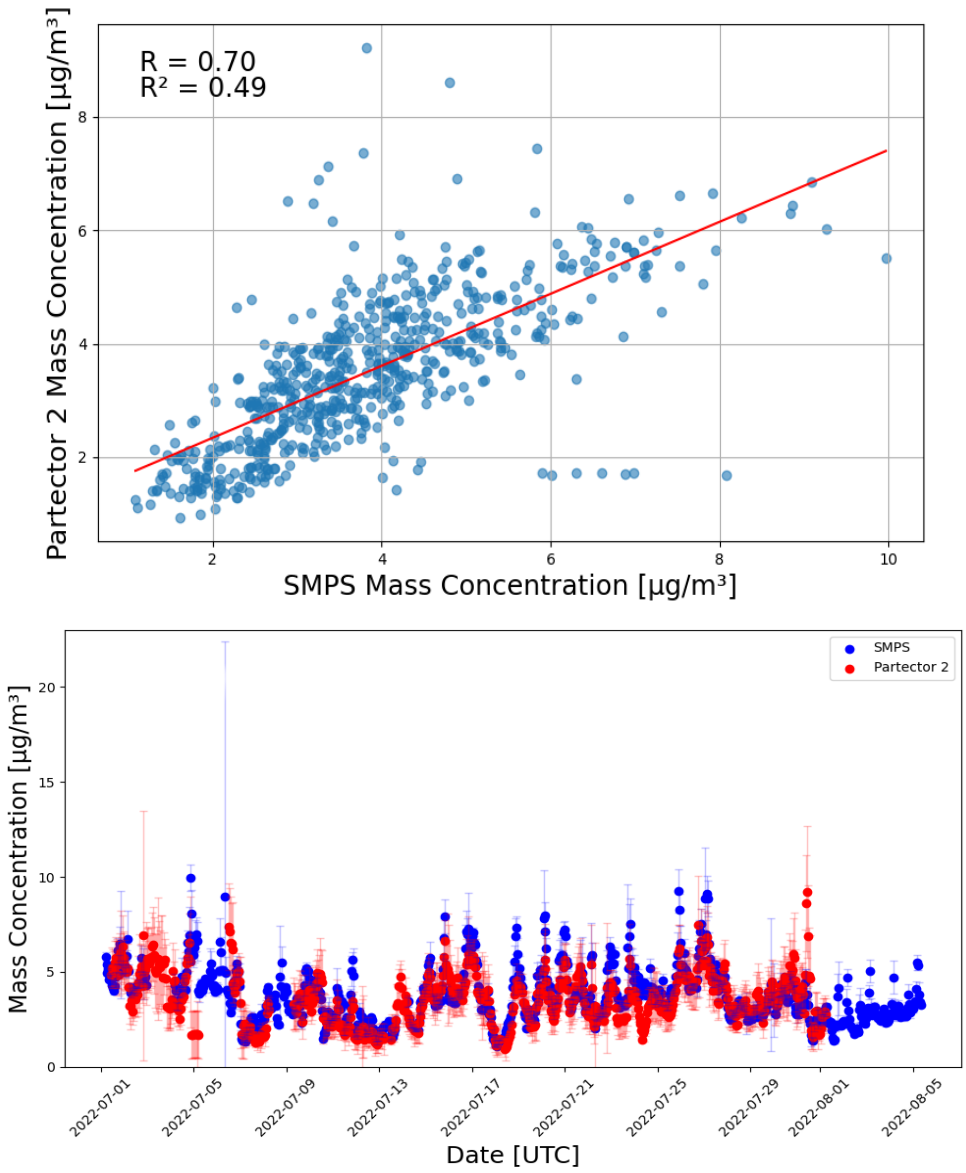

Fig. 2. Correlation between mass concentration measured by Partector 2 and SMPS at MARS site in July 2022 (colour online)

3.2. Mobile campaign measurements

In Table 2, in the comparison between the two seasons, we observe that the values of the mass concentration are similar, while the values of the particle number concentration and the LDSA have higher values in the cold period compared to the warm period. The large variation in particle number concentration between seasons is due to the fact that the cold period is dominated by ultrafine particles with smaller diameters than the ultrafine particles in the warm period [77].

The smaller diameter particle concentrations in the cold season can be explained by more intensive use of home heating during the winter, which contributes to the emission of ultrafine particles. Large quantities of these particles, which tend to be smaller and more numerous, contribute to higher particle number concentrations and LDSA. These particles may have smaller sizes during the cold period due to incomplete combustion processes [65]. During the cold period, the emitted particles are more likely to form in smaller sizes because the nucleation and condensation processes are favoured at low temperatures. Also, under low-temperature and high-pressure conditions, particles can remain suspended within the surface layer for longer periods, which contributes to higher mass and number concentrations [78]. Furthermore, during the cold period, higher traffic, possibly due to weather conditions that make road transport slower, may contribute to the emission of a higher number of ultrafine particles.

While the data in Table 2 shows differences in UFP number concentration and LDSA between the cold and warm periods, it is important to note the relatively high standard deviation; this suggests that the UFP values are highly dispersed. This dispersion indicates that the values around the mean are less frequent, which could imply that UFP concentrations are influenced by more localized or sporadic events, such as traffic peaks or specific heating activity, like was also emphasized by [79].

Table 2. Average value for each mobile campaigns and standard deviation

Period	Mass $PM_{0.3}$	No. conc.	Diameter	LDSA
Unit	$\mu g/m^3$	cm^{-3}	nm	$\mu m^2/cm^3$
Warm	10.5 ±13.2	27247 ±29337	46.7 ±10.6	59.7 ±46.5
Cold	10.7 ±12.7	47069 ±49913	41.7 ±14.4	75.2 ±59.1

$PM_{0.3}$ shows a high spatial variation in Bucharest, a characteristic mainly due to predominantly local sources. These particles are emitted mainly from point sources, such as road traffic, construction sites, and household activities, as well as from stationary sources such as industrial, commercial, or agricultural areas. Analysis of the measured data shows that the highest number concentrations of $PM_{0.3}$ are recorded in areas where the measurement campaign route intersects boulevards or streets with heavy traffic. This finding is in accordance with [80], which pinpoints that road traffic is one of the main sources of ultrafine particles.

As can be seen in Fig. 3, in addition to road traffic, residential areas contribute to the UFP number concentration, especially in the cold season, through the use of home heating systems. The yellow segments, visible in the right panel, are located in residential areas, mostly individual houses or small blocks of flats. Moreover, Fig. 3 shows that the western region of Bucharest registers the highest concentrations of UFP in both seasons. This can be explained in the warm season by the highest concentrations of UFP recorded in industrial areas, characterized by intense activities, as well as in areas with intense traffic (e.g., highways, Bucharest ring road, and main streets). Moreover, this region also includes most of the railway traffic from Bucharest. The highest concentrations of UFP in the western region of Bucharest during the cold season can be related to the existence of a large number of residential homes in this region (according to the INS [52], the western region has the highest density of houses in Bucharest). A significant increase in the maximum concentrations of the number concentration of UFP particles, especially of particles with very small diameters, was observed.

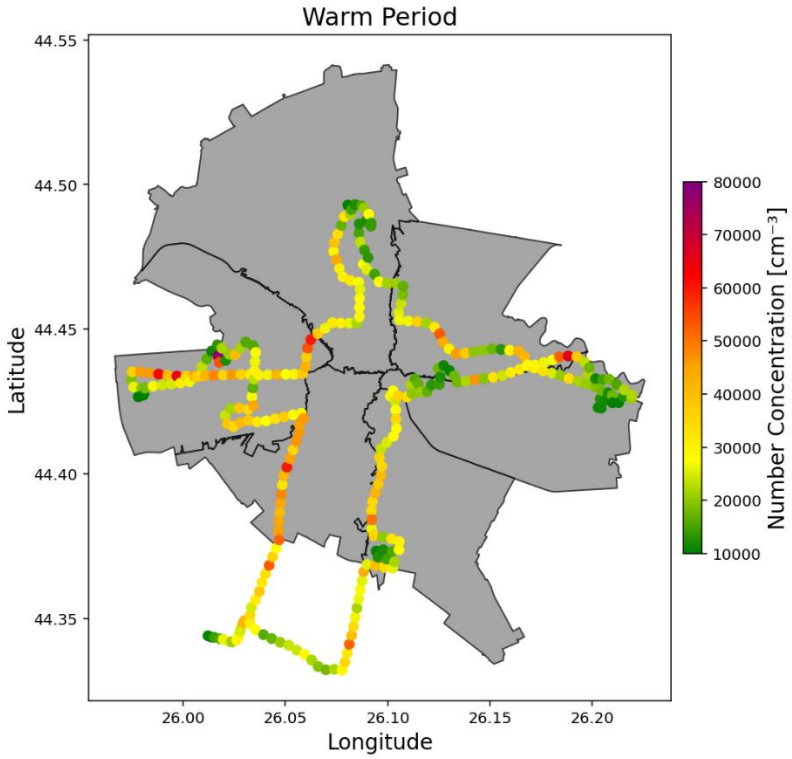

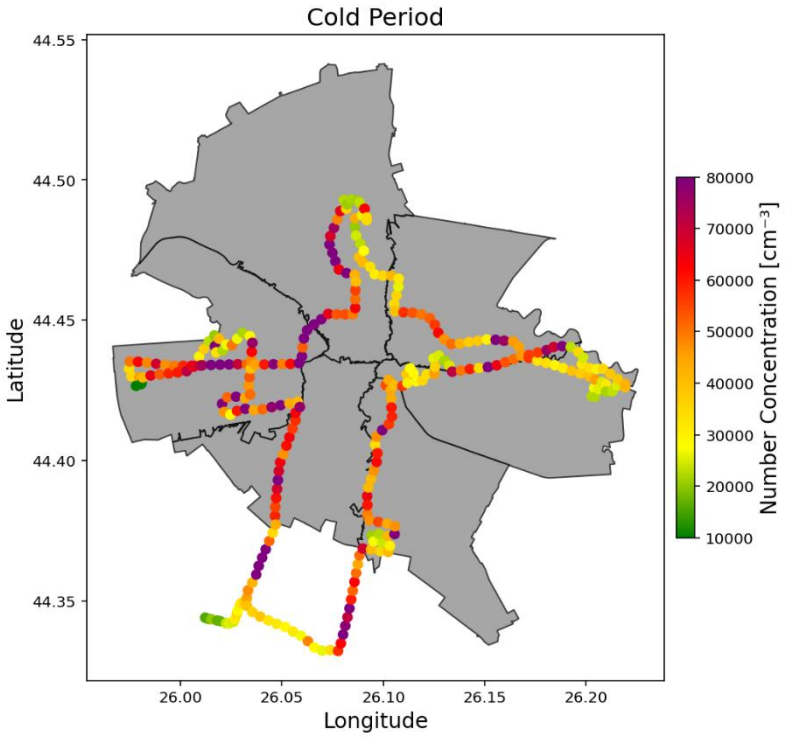

Fig. 3. Spatial variation of ultrafine particle number concentration in both seasons in Bucharest (colour online)

Fig. 4a represents the temporal variation of UFP number concentration between the two seasons, showing that particle concentrations are consistently higher during the cold period compared to the warm period. This suggests that, in addition to road traffic and industrial activities, meteorological factors (e.g., atmospheric pressure, temperature, solar radiation, or wind field) [81] and seasonal activities (e.g., agriculture and construction sites in the warm season or emissions due to home heating in the cold season) contribute to a greater increase of particles in the atmosphere as well as a varied dispersion of these particles depending on the sources that emit them. The large variability observed in Fig. 4a reflects a greater dependence of the number concentration of UFP particles on point sources (e.g., road traffic, residential heating) or on atmospheric factors (e.g., atmospheric pressure) than on stationary sources (i.e., industrial areas). Also, it can be seen that during the cold season the concentration of UFPs has higher values compared with the values measured during the warm season in most time intervals. This can be explained by the fact that during the cold season, home heating systems emit many more ultrafine particles of much smaller diameters that contribute to the increase in the number of particles compared to the warm season. Moreover, the atmospheric pressure regime during the cold season is higher (blue boxplots in Fig. 4b) which enables the maintenance of UFPs higher concentration values within the surface layer, compared with the warm season when the predominantly lower pressure regime (red box in Fig. 4b) favours the dispersion [82] of UFPs and consequently, the number concentration of UFPs is lower. The steep increase intervals in winter can be associated with the beginning of the day between 5 and 8 UTC, this being influenced by house heating and traffic.

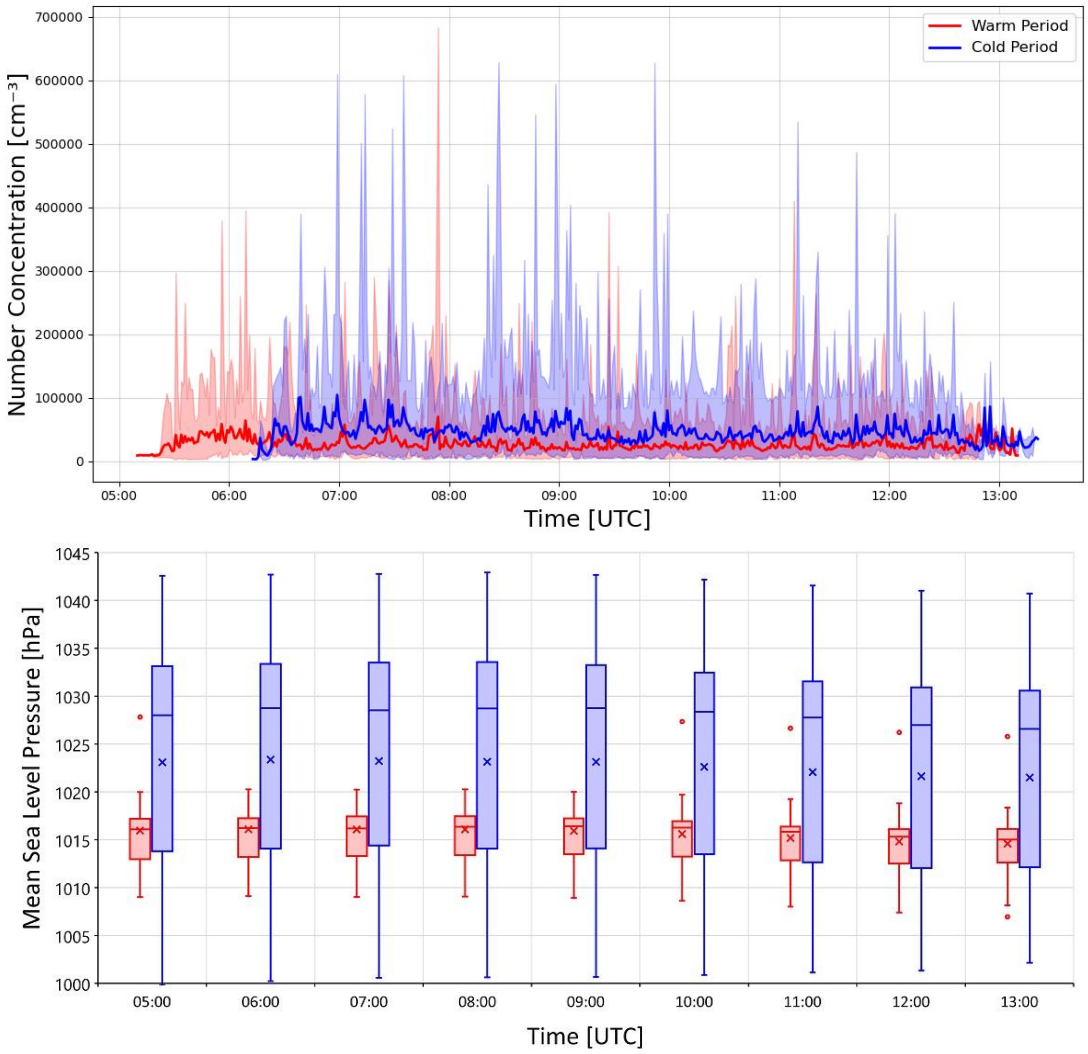

Fig. 4. (a) Temporal variation of number concentration during the warm (red line) and cold seasons (blue line), with error bars (shaded), represented by maximum and minimum values, and (b) hourly distribution of atmospheric pressure during the warm (red box) and cold seasons (blue box) (colour online)

Fig. 5 presents a comparative analysis of ultrafine particle number concentration measurements during the two campaign periods. The left panel illustrates data from the warm season, where UFP concentrations remain relatively moderate, predominantly ranging between 14,000 and 33,000 #cm^{-3}. The lowest recorded concentration, approximately 14,000 #cm^{-3}, was observed on 6th June, while the highest, reaching 33,000 #cm^{-3}, occurred on 26th May. Throughout this period, the concentrations exhibit relative stability without outliers, correlated with the low-pressure regime (Fig. 4b red boxes), which contribute to the dispersion processes

In contrast, the right panel displays data from the cold season, where UFP concentrations are significantly higher. Frequently exceeding 40,000 #cm^{-3} and occasionally surpassing 80,000 #cm^{-3}. The lowest recorded concentration, 22,400 #cm^{-3}, was observed on 18th January, while the highest peak, 85,000 #cm^{-3}, occurred on 21st February. This seasonal contrast suggests that UFP number concentrations are considerably elevated during winter, likely due to a combination of increased emissions from residential heating, lower atmospheric dispersion, and meteorological conditions (i.e., high pressure regime, shown by the blue box in Fig. 4b) which contributes to the accumulation of pollutants.

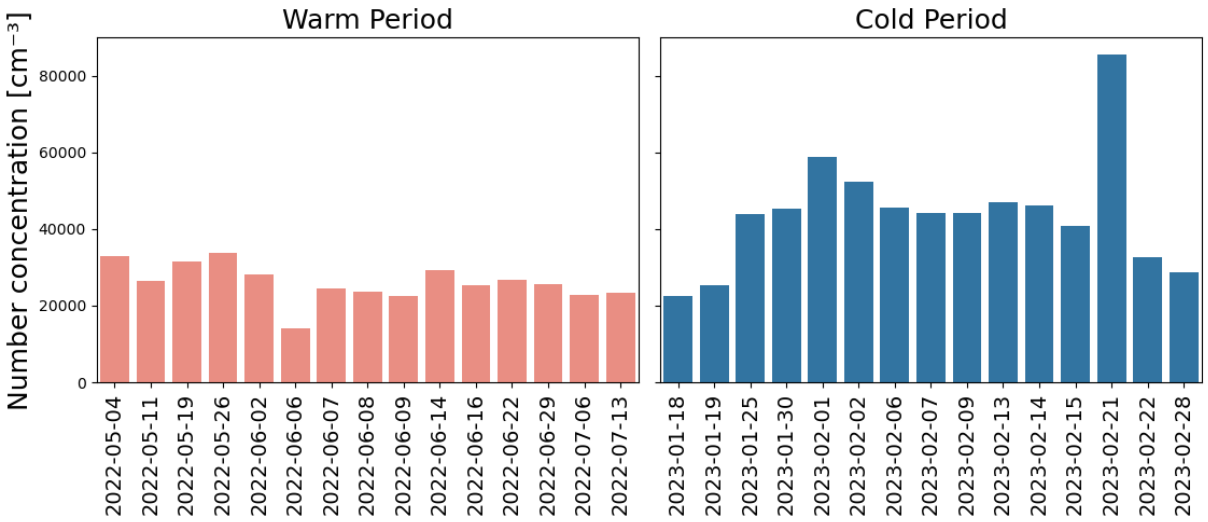

Fig. 5. Comparison of ultrafine particle (UFP) number concentrations measured during the warm season (May–July 2022) and cold season (January–February 2023) (colour online)

Fig. 6 shows the hourly mean for all days considered of the particle number concentrations during the two seasons. During the warm season, the normal distribution of the number concentration is broader and has higher maximum values than in winter, which indicates the presence of larger particles. During the warm season, the normal distribution is narrower, and the central values are more concentrated around 40-60 nm, while the particle distribution in winter at the beginning of the day starts with values ranging between 40 and 60 nm, but at noon the distribution develops into two lobes, one between 15-25 nm and the other between 50-60 nm, highlighting the presence of multiple particle sources.

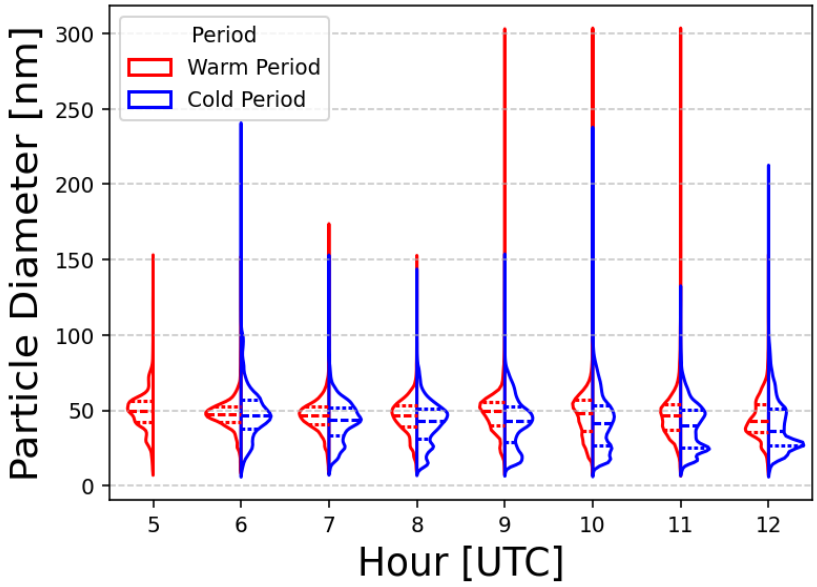

Fig. 6. Hourly particle diameter variation during the cold and warm seasons (colour online)

4. Shortcomings of the method

While the Partector 2 proved effective for mobile measurements, several challenges were encountered during our campaigns. A notable limitation was the influence of environmental factors, particularly vehicular traffic. Since measurements were conducted using a car on public streets, data were notably affected by traffic density, which varied by the time of day. High traffic volumes between 5:00 and 07:00 UTC on specific segments of the route introduced elevated particle counts, potentially overshadowing other environmental trends. This effect was less dependent on the location and more closely tied to temporal traffic patterns. However, it should be noted that the motivation of the study was to quantify the variability of UFP concentrations during the workdays and daytime on different levels of driveways, which of course imply capture of the traffic influence on the particle generation.

Another challenge was the dynamic nature of mobile measurements themselves. Changes in speed, proximity to exhaust sources, and temporary stops (e.g., traffic lights) could introduce variability in recorded values. Additionally, atmospheric conditions such as the pressure regime might have influenced particle dispersion and measurement consistency.

5. Conclusions

In this study we analysed the capabilities of Partector 2, an electronic aerosol dosimeter, to highlight the seasonal difference of ultrafine particle emissions and to identify the main sources of ultrafine particles in Bucharest.

Data provided by Partector 2 revealed significant variations in ultrafine particle concentrations between seasons, with higher particle number concentrations and LDSA values during the cold period compared to the warm period. This seasonal variation is likely driven by increased emissions from home heating and traffic during winter, which generate smaller and more numerous particles due to incomplete combustion and favourable nucleation conditions at low temperatures. Additionally, the high standard deviation in the data provided by Partector 2 suggests that UFP concentrations are influenced by sporadic events such as traffic peaks and localised heating activities, leading to a wider dispersion of values.

The results show that ultrafine particles have a high spatial variability in Bucharest, primarily influenced by local emission sources such as road traffic, industrial activities, and residential heating. In general, vehicle emissions are the main source of ultrafine particles, which is also confirmed by the data provided by Partector 2, which recorded the highest values of ultrafine particle concentrations along major traffic routes. In addition, the seasonal variations observed in the data provided by indicate that residential heating has an increased contribution to the number concentrations during winter, especially in the western region of Bucharest, which has the highest residential home density.

Significant diurnal variations in particle concentrations were also observed, especially in the cold season, with peaks occurring during morning and evening hours corresponding to traffic and heating activities. The warm season exhibited less pronounced diurnal variation, suggesting a more consistent emission pattern possibly influenced by factors like solar radiation and reduced seasonal heating or traffic.

The results of this study demonstrate that aerosol dosimeters, can be a reliable solution for air quality monitoring and characterisation in urban areas after a proper calibration and intercomparison with more robust technique to assess the level of uncertainties. Integrating such dosimeters into Romania's national air quality monitoring network would enhance the scientific understanding of ultrafine particle (UFP) dynamics in urban areas. Long-term monitoring and characterisation of UFP concentrations could provide valuable insights into their temporal variability, sources, and potential health impacts, supporting more informed air quality assessments and mitigation strategies.

Acknowledgements

Part of the work performed for this study was funded by the European Union's Horizon 2020 research and innovation programme through the ATMO-ACCESS Integrating Activity under grant agreement No 101008004 and by RI-URBANS project (Research Infrastructures Services Reinforcing Air Quality Monitoring Capacities in European Urban & Industrial Areas), European Union's Horizon 2020 research and innovation program under grant agreement, contract 101036245; and the Core Program within the National Research Development and Innovation Plan 2022–2027, carried out with the support of MCID, project no. PN 23 05.

References

[1] C. Bohren, D. Huffman, Absorption and scattering of light by small particles, John Wiley & Sons, 2008.
[2] E. Weingartner, H. Saathoff, M. Schnaiter, N. Streit, B. Bitnar, U. Baltensperger, Journal of Aerosol Science **34**(10), 1445 (2003).
[3] W. Solecki, D. Roberts, K. Seto, Nature Climate Change **14**, 685 (2024).
[4] EEA, Europe's air quality status 2024, European Environment Agency, Accessed: Dec. 05, 2024. [Online]. Available: https://www.eea.europa.eu//publications/europes-air-quality-status-2024
[5] N. V. S. Vallabani, O. Gruzieva, K. Elihn, A. Juárez Facio, S. Steimer, J. Kuhn, S. Silvergren, J. Portugal, B. Piña, U. Olofsson, C. Johansson, H. Karlsson, Environmental Research **231**, 116186 (2023).
[6] D. Schraufnagel, Experimental and Molecular Medicine **52**, 311 (2020).
[7] A. Ilie, J. Vasilescu, C. Talianu, C. Iojă, A. Nemuc, Atmosphere **14**(12), 1759 (2023).
[8] A. Iskandar, Z. Andersen, K. Bønnelykke, T. Ellermann, K. Andersen, H. Bisgaard, Thorax **67**, 252 (2011).
[9] U. Franck, S. Odeh, A. Wiedensohler, B. Wehner, O. Herbarth, The Science of the Total Environment **409**, 4217 (2011).
[10] K. Donaldson, V. Stone, A. Clouter, L. Renwick, W. MacNee, Occup. Environ. Med. **58**(3), 211 (2001).
[11] D. Kittelson, I. Khalek, J. McDonald, J. Stevens, R. Giannelli, Journal of Aerosol Science **159**, 105881 (2022).
[12] J. Marra, J. Phys.: Conf. Ser. **304**, 012010 (2011).

[13] V. Kumar, Statistical Learning and Modeling of Low-Cost Air Quality Sensor Data and Epidemiological Analysis, 2023.
[14] J. A. Marval Diaz, P. Tronville, Building and Environment **216**, 108992 (2022).
[15] H. Wu, Z. Li, M. Jiang, C.-S. Liang, D. Zhang, T. Wu, Y. Wang, M. Cribb, Atmospheric Environment **262**, 118652 (2021).
[16] M. Kulmala, Science **302**, 1000 (2003).
[17] European Union, Directive (EU) 2024/2881 of the European Parliament and of the Council of 23 October 2024 on ambient air quality and cleaner air for Europe (recast), EU, Oct. 24, 2024. Accessed: Feb. 17, 2025. [Online]. Available: https://eur-lex.europa.eu/eli/dir/2024/2881/oj
[18] C. Alpopi, S. Colesca, Theoretical and Empirical Researches in Urban Management **5**, 92 (2010).
[19] A. Cohen, H. R. Anderson, B. P. K. Ostro, M. Krzyzanowski, N. Künzli, K. Gutschmidt, Comparative Quantification of Health Risks: Global and Regional Burden of Disease Attributable to Selected Major Risk Factors, 1353 (2004).
[20] A. Piracha, M. Chaudhary, Sustainability **14**, 9234 (2022).
[21] C. Reche, M. Viana, I. Rivas, L. Bouso, M. Alvarez-Pedrerol, A. Alastuey, J. Sunyer, X. Querol, The Science of the Total Environment **493C**, 943 (2014).
[22] M. Hachem, N. Saleh, L. Bensefa-Colas, I. Momas, Indoor Air **31**, 2020.
[23] M. Manigrasso, P. Avino, C. Fanizza, Fresenius Environmental Bulletin **18**, 1341 (2009).
[24] J. Hofman, J. Staelens, R. Cordell, C. Stroobants, N. Zíková, S. Hama, K. Wyche, G. Kos, S. van der Zee, K. Smallbone, E. Weijers, P. Monks, E. Roekens, Atmospheric Environment **136**, 68 (2016).
[25] D. Wu, T. Xiao, X. Liao, J. Luo, C. Wu, S. Zhang, Y. Li, Y. Guo, Proceedings of the ACM on Interactive, Mobile, Wearable and Ubiquitous Technologies **4**, 1 (2020).
[26] A. Samad, U. Vogt, Atmospheric Environment **244**, 2021.
[27] J. Gomez, P. Arroyo, R. Alfonso, J. I. Suárez, E. Pinilla-Gil, J. Lozano, Sensors **22**, 1272 (2022).
[28] S. Kaivonen, E. Ngai, Digital Communications and Networks **6**, 2019.
[29] I. Pigliautile, G. Marseglia, A. L. Pisello, Sustainability **12**, 3936 (2020).
[30] H. Lv, H. Li, Z. Qiu, F. Zhang, J. Song, Atmospheric Pollution Research **12**, 112 (2021).
[31] M. Schaefer, H. Ebrahimi Salari, H. Köckler, N. Thinh, Science of the Total Environment **794**, 148709 (2021).
[32] A. Spira-Cohen, L.-C. Chen, M. Kendall, R. Sheesley, Journal of Exposure Science and Environmental Epidemiology **20**, 446 (2009).
[33] L. Morawska, T. Phong, X. Liu, A. Asumadu-Sakyi, G. Ayoko, A. Bartonova, A. Bedini, F. Chai, B. Christensen, M. Dunbabin, J. Gao, G. Hagler, R. Jayaratne, P. Kumar, A. Lau, P. Louie, M. Mazaheri, Z. Ning, N. Motta, R. Williams, Environment International **116**, 286 (2018).
[34] M. Zuurbier, G. Hoek, M. Oldenwening, V. Lenters, K. Meliefste, P. Hazel, B. Brunekreef, Environmental Health Perspectives **118**, 783 (2010).
[35] A. Nazelle, O. Bode, J. Orjuela, Environment International **99**, 151 (2016).
[36] M. Van Poppel, J. Peters, N. Bleux, Environmental Pollution **183**, 224 (2013).
[37] S. Devarakonda, P. Sevusu, H. Liu, R. Liu, L. Iftode, B. Nath, UrbComp '13: Proceedings of the 2nd ACM SIGKDD International Workshop on Urban Computing, 1 (2013).
[38] P. Macnaughton, S. Melly, J. Vallarino, G. Adamkiewicz, J. Spengler, The Science of the Total Environment **490C**, 37 (2014).
[39] X. Liu, J. Schnelle-Kreis, Z. Xun, J. Bendl, M. Khedr, G. Jakobi, B. Hai, J. Hovorka, R. Zimmermann, Science of the Total Environment **722**, 137632 (2020).
[40] A. Singh, D. Nganga, M. Gichuru, A. Weldetinsae, + Z. A. Alemu, N. Derrick, M. Webster, S. Bartington, G. N. Thomas, W. Avis, F. Pope, Environmental Research Communications **3**, 075007 (2021).
[41] S. Wang, Y. Ma, Z. Wang, L. Wang, X. Chi, A. Ding, M. Yao, Y. Li, Q. Li, M. Wu, L. Zhang, Y. Xiao, Y. Zhang, Atmospheric Chemistry and Physics **21**, 7199 (2021).
[42] Y. Liu, Y. Jiang, M. Wu, S. Muheyat, D. Yao, X. Jin, Environmental Science and Pollution Research **29**, 1 (2022).
[43] J. Kerckhoffs, J. Khan, G. Hoek, Z. Yuan, T. Ellermann, O. Hertel, M. Ketzel, S. S. Jensen, K. Meliefste, R. Vermeulen, Environmental Science and Technology **56**(11), 7174 (2022).
[44] D. Ranasinghe, W. Choi, A. Winer, S. Paulson, Aerosol and Air Quality Research **16**, 1841 (2016).
[45] M. Guevara, C. Tena Medina, A. Soret, K. Serradell, D. Guzmán, A. Retama, P. Camacho, M. Jaimes, A. Mediavilla-Sahagun, Science of the Total Environment **584**, 2017.
[46] L. Giovannini, E. Ferrero, T. Karl, M. Rotach, C. Staquet, S. Trini Castelli, D. Zardi, Atmosphere **11**, 646 (2020).
[47] J. Van den Bossche, J. Peters, J. Verwaeren, D. Botteldooren, J. Theunis, B. De Baets, Atmospheric Environment **105**, 148 (2015).
[48] U. Vito, 'Deliverable D13 (D2. 5)', 2022.
[49] D. Hagan, J. H. Kroll, Atmospheric Measurement Techniques **13**, 6343 (2020).
[50] J. Kerckhoffs, G. Hoek, U. Gehring, R. Vermeulen, Environment International **154**, 106569 (2021).
[51] M. Fierz, D. Meier, P. Steigmeier, H. Burtscher, Aerosol Science and Technology **48**, 350 (2014).
[52] INSSE, National Institute of Statistics. Accessed:

Apr. 08, 2024. [Online]. Available: https://insse.ro/cms/en
[53] N. Barbu, C. Burada, S. Stefan, F. Georgescu, Acta Geophysica **64**,510 (2016).
[54] S. Andrei, F. Toanca, A. Dandocsi, L. Belegante, A. Nemuc, L. Marmureanu, V. Vulturescu, G. Florescu, D. Nicolae, J. Optoelectron. Adv. M. **19**(9–10), 610 (2017).
[55] I. A. Nita, L. Apostol, C. Patriche, L. Sfica, R. Bojariu, M. V. Birsan, Romanian Journal of Physics **67**, 812 (2022).
[56] A. Manea, M.-V. Birsan, V. Dima, L.-E. Havriș, Land **13**(5), 596 (2024).
[57] L. Mărmureanu, J. Vasilescu, J. Slowik, A. S. H. Prévôt, C. A. Marin, B. Antonescu, A. Vlachou, A. Nemuc, A. Dandocsi, S. Szidat, Atmosphere **11**(4), 385 (2020).
[58] D. Nicolae, C. Talianu, J. Ciuciu, M. Ciobanu, V. Babin, J. Optoelectron. Adv. M. **8**(1), 238 (2006).
[59] Urban Air Pollution - European Aspects, J. Fenger, O. Hertel, F. Palmgren eds., Springer Science + Business Media, B. V., 1998.
[60] C. Talianu, J. Vasilescu, D. Nicolae, A. Ilie, A. Dandocsi, A. Nemuc, L. Belegante, Atmospheric Chemistry and Physics **25**(9), 4639 (2025).
[61] R. Pîrloagă, M. Adam, B. Antonescu, S. Andrei, S. Ştefan, Remote Sensing **15**(6), 1514 (2023).
[62] B. Livio, C. Talianu, A. Nemuc, V. Nicolae, G. Ciocan, F. Toanca, O. Tudose, C. Radu, D. Nicolae, J. Optoelectron. Adv. M. **26**(9-10), 422 (2024).
[63] V. Nicolae, O.-G. Tudose, L. Belegante, J. Vasilescu, A. Nemuc, F. Toanca, D. Nicolae, C. Radu, J. Optoelectron. Adv. M. **25**(3-4), 176 (2023).
[64] P. Laj, C. Lund Myhre, V. Riffault, V. Amiridis, H. Fuchs, K. Eleftheriadis, T. Petäjä, T. Salameh, N. Kivekäs, E. Juurola, G. Saponaro, S. Philippin, C. Cornacchia, L. Alados Arboledas, H. Baars, A. Claude, M. De Mazière, B. Dils, M. Dufresne, N. Evangeliou, O. Favez, M. Fiebig, M. Haeffelin, H. Herrmann, K. Höhler, N. Illmann, A. Kreuter, E. Ludewig, E. Marinou, O. Möhler, L. Mona, L. Eder Murberg, D. Nicolae, A. Novelli, E. O'Connor, K. Ohneiser, R. M. Petracca Altieri, B. Picquet-Varrault, D. Van Pinxteren, B. Pospichal, J.-P. Putaud, S. Reimann, N. Siomos, I. Stachlewska, R. Tillmann, K. A. Voudouri, U. Wandinger, A. Wiedensohler, A. Apituley, A. Comerón, M. Gysel-Beer, N. Mihalopoulos, N. Nikolova, A. Pietruczuk, S. Sauvage, J. Sciare, H. Skov, T. Svendby, E. Swietlicki, D. Tonev, G. Vaughan, V. Zdimal, U. Baltensperger, J.-F. Doussin, M. Kulmala, G. Pappalardo, S. Sorvari Sundet, M. Vana, Bulletin of the American Meteorological Society **105**(7), E1098 (2024).
[65] K. Sartelet, J. Kerckhoffs, E. Athanasopoulou, L. Lugon, J. Vasilescu, J. Zhong, G. Hoek, C. Joly, S.-J. Park, C. Talianu, S. Van Den Elshout, F. Dugay, E. Gerasopoulos, A. Ilie, Y. Kim, D. Nicolae, R. M. Harrison, T. Petäjä, Environment International **199**, 109474 (2025).
[66] A. Todea, S. Beckmann, H. Kaminski, D. Bard, S. Bau, S. Clavaguera, D. Dahmann, H. Dozol, N. Dziurowitz, K. Elihn, M. Fierz, G. lidén, A. Meyer-Plath, C. Monz, V. Neumann, J. Pelzer, B. Simonow, P. Thali, I. Tuinman, C. Asbach, The Science of the Total Environment **605–606**, 929 (2017).
[67] M. Fierz, C. Houle, P. Steigmeier, H. Burtscher, Aerosol Science and Technology **45**, 1 (2011).
[68] J. Marra, M. Voetz, H.-J. Kiesling, Journal of Nanoparticle Research **12**, 21 (2010).
[69] A. Wiedensohler, W. Birmili, A. Nowak, A. Sonntag, K. Weinhold, M. Merkel, B. Wehner, T. Tuch, S. Pfeifer, M. Fiebig, A. M. Fjäraa, E. Asmi, K. Sellegri, R. Depuy, H. Venzac, P. Villani, P. Laj, P. Aalto, J. A. Ogren, E. Swietlicki, P. Williams, P. Roldin, P. Quincey, C. Hüglin, R. Fierz-Schmidhauser, M. Gysel, E. Weingartner, F. Riccobono, S. Santos, C. Grüning, K. Faloon, D. Beddows, R. Harrison, C. Monahan, S. G. Jennings, C. D. O'Dowd, A. Marinoni, H.-G. Horn, L. Keck, J. Jiang, J. Scheckman, P. H. McMurry, Z. Deng, C. S. Zhao, M. Moerman, B. Henzing, G. De Leeuw, G. Löschau, S. Bastian, Atmos. Meas. Tech. **5**(3), 657 (2012).
[70] TSI, Condensation Particle Counter, TSI, Apr. 01, 2022.
[71] J. Kerckhoffs, PhD Thesis, Utrecht University, 2021.
[72] TomTom, Bucharest Traffic. Accessed: Mar. 06, 2025. [Online]. Available: https://www.tomtom.com/traffic-index/bucharest-traffic/
[73] J. Van Den Bossche, K. Jordahl, M. Fleischmann, J. McBride, J. Wasserman, M. Richards, A. G. Badaracco, A. D. Snow, J. Tratner, J. Gerard, B. Ward, M. Perry, C. Farmer, G. A. Hjelle, M. Taves, E. T. Hoeven, M. Cochran, Rraymondgh, S. Gillies, G. Caria, L. Culbertson, M. Bartos, N. Eubank, R. Bell, Sangarshanan, J. Flavin, S. Rey, Maxalbert, A. Bilogur, C. Ren, geopandas/geopandas: v0.13.2. (Jun. 06, 2023), Zenodo.
[74] T. Lepistö, H. Lintusaari, L. Salo, V. Silvonen, L. M. F. Barreira, J. Hoivala, L. Markkula, J. V. Niemi, J. Ondracek, K. Teinilä, H. E. Manninen, S. Saarikoski, H. Timonen, M. Dal Maso, T. Rönkkö, Aerosol Research **2**(2), 271 (2024).
[75] J. Löndahl, W. Möller, J. H. Pagels, W. G. Kreyling, E. Swietlicki, O. Schmid, Journal of Aerosol Medicine and Pulmonary Drug Delivery **27**(4), 229 (2014).
[76] P. McMurry, Atmospheric Environment **34**(12-14), 1959 (2000).
[77] Y. Wang, P. K. Hopke, M. J. Utell, Water Air Soil Pollut. **223**(5), 2223 (2012).
[78] S. A. Romshoo, M. A. Bhat, G. Beig, Science of the

Total Environment **799**, 149364 (2021).
[79] J. Kaur, C. Jhamaria, S. Tiwari, D. Singh Bisht, Nat. Env. Poll. Tech. **21**(2), 589 (2022).
[80] P. Kumar, L. Morawska, W. Birmili, P. Paasonen, M. Hu, M. Kulmala, R. Harrison, L. Norford, R. Britter, Environment International **66**, 1 (2014).
[81] E. Carstea, K. Fragkos, Optoelectron. Adv. Mat. **18**(11–12), 562 (2024).
[82] C. Talianu, D. Nicolae, J. Ciuciu, M. Ciobanu, V. Babin, J. Optoelectron. Adv. M. **8**(1), 243 (2006)

*Corresponding author: camelia@inoe.ro